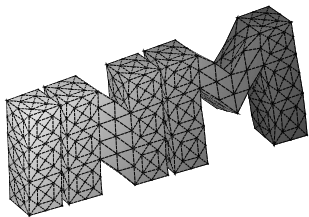# Technische Universität Graz

An algebraic multigrid method for an adaptive space–time finite element discretization

O. Steinbach, H. Yang

**Berichte aus dem
Institut für Numerische Mathematik**

Technische Universität Graz

An algebraic multigrid method for an adaptive space–time finite element discretization

O. Steinbach, H. Yang

Berichte aus dem Institut für Numerische Mathematik

Technische Universität Graz
Institut für Numerische Mathematik
Steyrergasse 30
A 8010 Graz

WWW: `http://www.numerik.math.tu-graz.ac.at`

An algebraic multigrid method for an adaptive space–time finite element discretization

Olaf Steinbach and Huidong Yang

Institut für Numerische Mathematik, Technische Universität Graz,
Steyrergasse 30, 8010 Graz, Austria
o.steinbach@tugraz.at and hyang@math.tugraz.at

Abstract. This work is devoted to numerical studies on an algebraic multigrid preconditioned GMRES method for solving the linear algebraic equations arising from an space–time finite element discretization of the heat equation using h–adaptivity on tetrahedral meshes. The finite element discretization is based on a Galerkin–Petrov variational formulation using piecewise linear finite elements simultaneously in space and time. In this work, we will focus on h–adaptivity relying on a residual based a posteriori error estimation, and we study some important components in the algebraic multigrid method for solving the space–time finite element equations.

Keywords: adaptive space–time finite element, algebraic multigrid

1 Introduction

The space–time finite element method has a long history since the starting work for the application in elastodynamics [11]. Recently, in [10, 16, 17], the authors have proposed a discontinuous Galerkin space–time finite element approach and robust multigrid methods for parabolic problems. In [12], space–time isogeometric analysis discretization methods for parabolic evolution equations in fixed and moving spatial computational domains have been investigated. In [3], the classical streamline–diffusion and edge averaged finite element method for time dependent convection–diffusion problems is considered. In [7, 8], space–time discontinuous Petrov–Galerkin finite elements with optimal test functions for fluid problems have been exploited. Further, a class of methods based on well–known space–time tensor product ansatz spaces can be found in, e.g., [1, 19, 22].

In this work, we follow the Galerkin–Petrov space–time finite element method recently proposed and analyzed in [20] for solving the model heat equation

$$\alpha\partial_t u(x,t) - \Delta_x u(x,t) = f(x,t) \quad \text{for } (x,t) \in Q := \Omega \times (0,T), \qquad (1)$$

with the boundary and initial conditions $u(x,t) = 0$ for $(x,t) \in \Sigma := \partial\Omega \times (0,T)$ and $u(x,0) = u_0$ for $x \in \Omega$, respectively. Here, $\Omega \subset \mathbb{R}^2$, is a bounded Lipschitz domain, and $\alpha \in \mathbb{R}_+$ is the heat capacity constant.

The Galerkin–Petrov variational formulation for the heat equation (1) is to find $\overline{u} \in X := \{v \in L^2(0,T;H_0^1(\Omega)) \cap H^1(0,T;H^{-1}(\Omega)), v(x,0) = 0 \text{ for } x \in \Omega\}$ such that

$$a(\overline{u},v) = \langle f,v \rangle - a(\overline{u}_0,v) \tag{2}$$

is satisfied for all $v \in Y := L^2(0,T;H_0^1(\Omega))$, where

$$a(u,v) := \int_0^T \int_\Omega \left[\alpha \partial_t u(x,t) v(x,t) + \nabla_x u(x,t) \cdot \nabla_x v(x,t) \right] dx\, dt,$$

$$\langle f,v \rangle := \int_0^T \int_\Omega f(x,t) v(x,t)\, dx\, dt,$$

and $\overline{u}_0 \in L^2(0,T;H_0^1(\Omega)) \cap H^1(0,T;H^{-1}(\Omega))$ denotes an arbitrary but fixed extension of the initial datum $u_0 \in H_0^1(\Omega)$. Existence and uniqueness of the solution to (2) is provided in [20], see also [19, 22].

The related discrete Galerkin–Petrov problem is to find $\overline{u}_h \in X_h \subset X$ such that

$$a(\overline{u}_h,v_h) = \langle f,v_h \rangle - a(\overline{u}_0,v_h) \tag{3}$$

is satisfied for all $v_h \in Y_h \subset Y$ where we assume $X_h \subset Y_h$. Then, the discrete inf–sup condition was shown in [20], from which we conclude a standard stability and error analysis.

In particular, the space–time cylinder Q is decomposed into finite elements $Q_h = \cup_{\ell=1}^N \overline{q}_\ell$. For simplicity we assume that Ω is polygonal bounded, $\overline{Q} = Q_h$. The finite element spaces are given by $X_h = S_h^1(Q_h) \cap X$ and $Y_h = X_h$ with $S_h^1(Q_h) = \mathrm{span}\{\varphi_i\}_{i=1}^M$ being the span of piecewise linear and continuous basis functions φ_i. The following energy error estimate is shown in [20],

$$\|\overline{u} - \overline{u}_h\|_{L^2(0,T;H_0^1(\Omega))} \le c\, h\, |\overline{u}|_{H^2(Q)}, \tag{4}$$

where $\overline{u} \in X$ and $\overline{u}_h \in X_h$ denote the unique solutions of the variational problems (2) and (3), respectively, $c > 0$ is a constant independent of the mesh size h, and we assume $\overline{u} \in H^2(Q)$.

In comparison with other space–time methods, this approach is very suitable for the development of h–adaptivity simultaneously in space and time, and we may further pose the question how to solve the arising linear system of equations, that will be tackled by an algebraic multigrid (AMG) preconditioned GMRES method.

The remainder of this paper is organized as follows: In Section 2 we discuss the space–time adaptive approach while Section 3 deals with the algebraic multigrid method for the finite element equations. Some numerical experiments are prescribed in Section 4. Finally, some conclusions are drawn in Section 5.

2   Space–time adaptivity

2.1   Local error indicator

Let $\overline{u}_h \in X_h$ be the space–time finite element solution of the variational problem (3) implying $u_h := \overline{u}_0 + \overline{u}_h$ for which we can define the local residuals

$$R_{q_\ell}(u_h) := f + \Delta_x u_h - \alpha \partial_t u_h$$

on each tetrahedral element q_ℓ and the jumps

$$J_\gamma(u_h) := [n_x \cdot \nabla_x u_h]_{|\gamma}$$

of the normal flux in spatial direction across the inner boundaries γ between q_ℓ and its neighbouring elements. The local error indicator on each element q_ℓ is then given as

$$\eta_{q_\ell} = \left\{ c_1 h_{q_\ell}^2 \|R_{q_\ell}\|_{L_2(q_\ell)}^2 + c_2 h_{q_\ell} \|J_\gamma\|_{L_2(\partial q_\ell)}^2 \right\}^{\frac{1}{2}}, \tag{5}$$

with suitable chosen positive constants c_1, c_2. For more details, we refer to our recent work [21]. In comparison with more conventional adaptive methods for time dependent problems, see, e.g., [9, 14, 15], our method allows us to perform the spatial and temporal adaptivity simultaneously.

2.2   Adaptive mesh refinement

Two local mesh refinement methods on the tetrahedral meshes Q_h have been employed in order to perform the space–time adaptivity, namely, the octasection based method [4], and the newest vertex bisection based method [2]. In the octasection based method, the marked tetrahedral elements are refined using a regular refinement [24], the handing nodes are closed by the so–called irregular refinement with 62 possible cases. It is important that the irregular elements will never be further refined on the next refinement levels in order to keep shape regularity of the tetrahedral elements. If such irregular elements are marked for a further refinement, we have to return to their parents, which are regular, and perform the regular refinement on these parental elements, and irregular refinement on those affected neighbouring elements. In the newest vertex bisection based method, the local refinement pattern for each tetrahedral element is fixed a priori following certain rules. In [2], there exist 5 refinement patterns defined for tetrahedral elements. The local refinement strictly follows the natural rules from one pattern to another. The closure of hanging nodes is realized by calling such local refinement recursively until no more hanging nodes exist.

2.3   The adaptive space–time finite element loop

The adaptive space–time finite element loop follows the standard adaptive finite element loop, see, e.g., [23], that consists of the following four main steps: Given a conforming decomposition Q_0 on the initial mesh level $k = 0$,

1. SOLVE: *Solve the discrete problem (3) on the adaptive mesh level k,*
2. ESTIMATE: *Compute the local error indicators (5) on each element q_ℓ,*
3. MARK: *Mark the elements for refinement using a proper marking strategy,*
4. REFINE: *Perform the local mesh refinement using octasection or bisection, increase level $k := k + 1$, obtain the conforming decomposition Q^k, and go to Step 1 if the solution is not accurate enough.*

In particular, for the module MARK, we use the Dörfler marking strategy [6]: For a given parameter $\theta \in [0, 1]$, find N_k such that

$$\theta \sum_{\ell=1}^{N_k} \eta_{q_\ell} \geq \sum_{\ell=1}^{M_k} \eta_{q_\ell},$$

where M_k denotes the total number of tetrahedral elements on the current level k. In order to mark as few elements as possible, it is desirable to hold $q_\ell \geq q_m$ if $\ell < m$. The tetrahedral elements with index from 1 to N_k will be marked for the refinement on the next level $k + 1$. In our numerical experiments, $\theta = 0.5$.

3   The algebraic multigrid method

The remaining task is to solve the linear system of algebraic equations arising from the space–time finite element discretization of the Galerkin–Petrov problem (3). It is clear that the stiffness matrix is not symmetric but positive definite. Hence we develop an AMG preconditioner for the GMRES method, that requires special care for its components, namely, the coarsening and smoother. So far, we have considered a greedy strategy for coarse–grid selection [13]. After the selection of coarse and fine grids. the interpolation matrix is defined as in classical AMG [5]. As a smoother, we employ the ω—Kaczmarz relaxation which satisfies the algebraic smoothing property [18]. More details on the development of the robust AMG method for such space–time finite element equations will be provided in a near future report.

4   Numerical experiments

4.1   Convergence history

As numerical example we consider $\Omega = (0,1)^2$ and $T = 1$, i.e. $Q = (0,1)^3$, and we chose a sufficiently smooth solution u given as

$$u(x,t) = (x_1^2 - x_1)(x_2^2 - x_2)(t^2 - t)e^{-100.0((x_1-0.25)^2+(x_2-0.25)^2+(t-0.25)^2)}. \quad (6)$$

To verify the estimated order of convergence (eoc), the $L^2(0,T;H_0^1(\Omega))$–norm of the error $e_h := u - u_h$ between the given and the discrete solution is calculated on five uniformly refined mesh levels L_1–L_5 with increasing number of degrees of freedom (#Dof) and tetrahedral elements (#Tet), and deceasing mesh size h. The mesh information is prescribed in Table 1.

Level	L_1	L_2	L_3	L_4	L_5
#Dof	125	729	4913	35937	274625
#Tet	384	3072	24586	196608	1572864
h	0.25	0.125	0.0625	0.03125	0.015625

Table 1. Mesh information on five uniformly refined levels.

The convergence results are recorded in Table 2 for varying heat conductivity parameters $\alpha = 1$, $\alpha = 10$, and $\alpha = 100$. From the numerical results we observe a linear order of convergence as predicted. The convergence history of the space–time finite element method using an adaptive mesh refinement in comparison with the uniform one is plotted in Figure 1 for $\alpha = 1$. The adaptive mesh always starts from the L_1 mesh level. To reach the same accuracy as the uniformly refinement, the two adaptive methods require much fewer degrees of freedom. Further, they provide a linear order of convergence.

Level	$\alpha = 1$		$\alpha = 10$		$\alpha = 100$	
	$\|e_h\|_{L_2(0,T;H_0^1(\Omega))}$	eoc	$\|e_h\|_{L_2(0,T;H_0^1(\Omega))}$	eoc	$\|e_h\|_{L_2(0,T;H_0^1(\Omega))}$	eoc
L_1	$3.77 \cdot 10^{-3}$	–	$3.78 \cdot 10^{-3}$	–	$4.10 \cdot 10^{-3}$	–
L_2	$2.93 \cdot 10^{-3}$	0.36	$3.01 \cdot 10^{-3}$	0.33	$4.21 \cdot 10^{-3}$	–
L_3	$2.00 \cdot 10^{-3}$	0.55	$2.04 \cdot 10^{-3}$	0.56	$2.36 \cdot 10^{-3}$	0.84
L_4	$1.07 \cdot 10^{-3}$	0.89	$1.08 \cdot 10^{-3}$	0.91	$1.13 \cdot 10^{-3}$	1.06
L_5	$5.47 \cdot 10^{-4}$	0.97	$5.49 \cdot 10^{-4}$	0.98	$5.56 \cdot 10^{-4}$	1.02

Table 2. The estimated order of convergence (eoc) on the mesh levels L_1–L_5 with different values for the heat conductivity: $\alpha = 1$, $\alpha = 10$, and $\alpha = 100$.
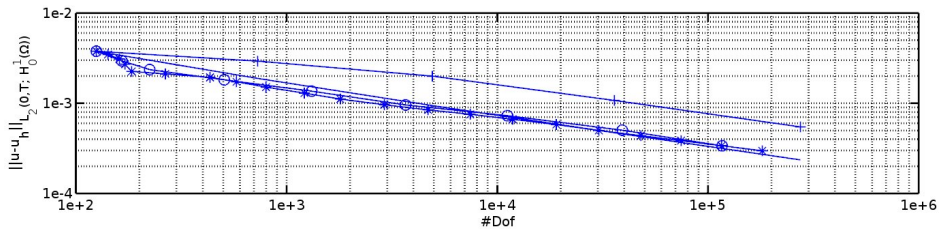

Fig. 1. Convergence history of the space–time finite element using a uniform and adaptive refinements: Uniform $(-+-)$, octasection $(-\circ-)$, bisection $(-*-)$ and linear $(-)$, for $\alpha = 1.0$.

4.2   AMG performance

To study the AMG performance, in Table 3 we show the number of AMG pre-conditioned GMRES iterations and the cost in seconds (s) for solving the model heat equation on uniformly refined five mesh levels (L_1–L_5). We set the relative residual error $\varepsilon = 10^{-7}$ as the stopping criterion for the GMRES iteration, and run $1-2$ AMG iterations in each preconditioning step. We observe a relatively fair robustness with respect to the mesh size h and heat capacity α.

α	L_1	L_2	L_3	L_4	L_5
1	3	4	7	14	32
10	2	4	6	14	24
100	3	4	6	9	15

α	L_1	L_2	L_3	L_4	L_5
1	0.001 s	0.032 s	0.373 s	7.437 s	143.190 s
10	0.001 s	0.033 s	0.667 s	9.171 s	190.070 s
100	0.001 s	0.060 s	1.383 s	27.060 s	448.590 s

Table 3. Performance of the AMG precontioned GMRES method on five uniform mesh levels: Number of GMRES iterations (left) and time in seconds (right).

In Figure 2 and Figure 3, respectively, we compare the computational time in seconds (s) and the number of AMG preconditioned GMRES iterations to reach the same accuracy of the space–time finite element solution between the adaptive and uniform refinements. In comparison with the uniform refinement, the adaptive one shows more efficiency in saving the number of AMG preconditioned GMRES iterations as well as in the computational time.
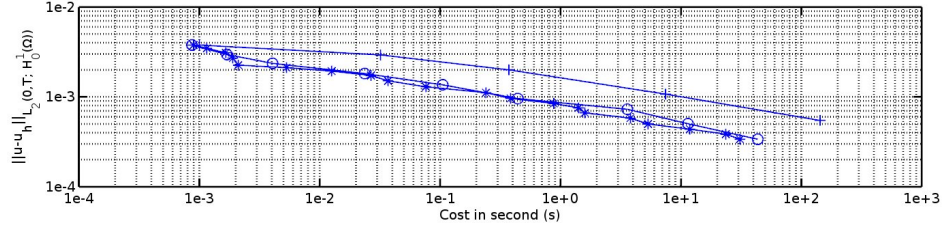

Fig. 2. Comparison of the computional cost in seconds (s) to reach the same accuracy of the space–time finite element solution using uniform and adaptive refinements: Uniform $(-+-)$, octasection $(-\circ-)$ and bisection $(-*-)$, for $\alpha = 1.0$.

4.3   Visualization

The visualization of the numerical solution and of the adaptive space–time meshes at three planes, in particular for $x_1 = 0.5$, $x_2 = 0.5$, and $t = 0.25$, are shown in Figure 4. It is easy to see that our adaptive methods capture the interest in the space–time domain effectively and make the adaptive mesh refinement in space and time simultaneously.
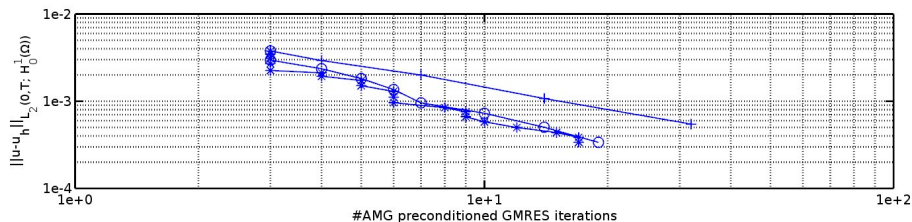
Fig. 3. Comparison of the AMG preconditioned GMRES iterations to reach the same accuracy of the space–time finite element solution using the uniform and adaptive refinements: Uniform $(- + -)$, octasection $(- \circ -)$ and bisection $(- * -)$, for $\alpha = 1.0$.
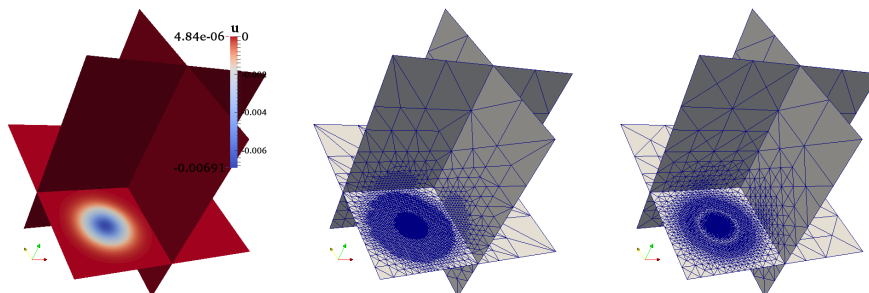

Fig. 4. Visualization of the numerical solution and of the adaptive space–time meshes at the three planes for $x_1 = 0.5$, $x_2 = 0.5$, and $t = 0.25$: Numerical solution (left), adaptive meshes using octasection at the 9th refinement level (middle) and bisection at the 19th refinement level (right).

5 Conclusions

In this work, we have developed an AMG preconditioned GMRES method for solving the adaptive space–time finite element discretized heat equation. The proposed method has demonstrated a relatively good performance with respect to the mesh size and heat capacity. The adaptive space–time finite element method has shown a better accuracy and performance than the uniform one with respect to the number of degrees of freedom and computational time, respectively. The ongoing work is to develop a fully robust AMG preconditioner with respect to the discetization, heat capacity, and more diffusion coefficients.

References

1. R. Andreev. Wavelet–in–time multigrid–in–space preconditioning of parabolic evolution equations. *SIAM J. Sci. Comput.*, 38(1):A216–A242, 2016.

2. D. N. Arnold, A. Mukherjee, and L. Pouly. Locally adapted tetrahedral meshes using bisection. *SIAM J. Sci. Comput.*, 22(2):431–448, 2000.
3. R. E. Bank, P. S. Vassilevski, and L. T. Zikatanov. Arbitrary dimension convection–diffusion schemes for space–time discretizations. *J. Comput. Appl. Math.*, 310:19–31, 2017.
4. J. Bey. Tetrahedral grid refinement. *Computing*, 55(4):355–378, 1995.
5. W. L. Briggs, V. E. Henson, and S. F. McCormick. *A multigrid tutorial.* SIAM, Philadelphia, 2000.
6. W. Dörfler. A convergent adaptive algorithm for Poisson's equation. *SIAM J. Numer. Anal.*, 33(3):1106–1124, 1996.
7. T. E. Ellis. *Space–time discontinuous Petrov–Galerkin finite elements for transient fluid mechanics.* PhD thesis, University of Texas at Austin, 2016.
8. T. E. Ellis, L. Demkowicz, and J. Chan. Locally conservative discontinuous Petrov–Galerkin finite elements for fluid problems. *Comput. & Math. Appl.*, 68(11):1530–1549, 2014.
9. K. Eriksson and C. Johnson. Adaptive finite element methods for parabolic problems I: A linear model problem. *SIAM J. Numer. Anal.*, 28(1):43–77, 1991.
10. M. J. Gander and M. Neumüller. Analysis of a new space–time parallel multigrid algorithm for parabolic problems. *SIAM J. Sci. Comput.*, 38(4):A2173–A2208, 2016.
11. T. J. R. Hughes and G. M. Hulbert. Space–time finite element methods for elastodynamics: Formulations and error estimates. *Comput. Methods Appl. Math.*, 66(3):339–363, 1988.
12. U. Langer, S. E. Moore, and M. Neumüller. Space–time isogeometric analysis of parabolic evolution problems. *Comput. Methods Appl. Math.*, 306:342–363, 2016.
13. S. MacLachlan and Y. Saad. A greedy strategy for coarse–grid selection. *SIAM J. Sci. Comput.*, 29(5):1825–1853, 2007.
14. D. Meidner and B. Vexler. Adaptive spacetime finite element methods for parabolic pptimization problems. *SIAM J. Control Optim.*, 46(1):116–142, 2007.
15. P. K. Moore. A posteriori error estimation with finite element semi– and fully discrete methods for nonlinear parabolic equations in one space dimension. *SIAM J. Numer. Anal.*, 31(1):149–169, 1994.
16. M. Neumüller. *Space–time methods: Fast solvers and applications.* PhD thesis, TU Graz, 2013.
17. M. Neumüller and O. Steinbach. Refinement of flexible space–time finite element meshes and discontinuous Galerkin methods. *Comput. Vis. Sci.*, 14:189–205, 2011.
18. C. Popa. Algebraic multigrid smoothing property of Kaczmarz's relaxation for general rectangular linear systems. *Electron. Trans. Numer. Anal.*, 29:150–162, 2007.
19. C. Schwab and R. Stevenson. Space–time adaptive wavelet methods for parabolic evolution problems. *Math. Comp.*, 78(267):1293–1318, 2009.
20. O. Steinbach. Space–time finite element methods for parabolic problems. *Comput. Methods Appl. Math.*, 15:551–566, 2015.
21. O. Steinbach and H. Yang. An adaptive space–time finite element method for solving the heat equation. Technical report, TU Graz, 2017. In preparation.
22. K. Urban and A. T. Patera. An improved error bound for reduced basis approximation of linear parabolic problems. *Math. Comp.*, 83(288):1599–1615, 2014.
23. R. Verfürth. *A Posteriori Error Estimation Techniques for Finite Element Methods.* Oxford Unversity Press, Oxford, 2013.
24. S. Zhang. *Multi–level Iterative Techniques.* PhD thesis, Penn State University, 1988.